Novel behaviour and structure of new glasses of the type Ba–Al–O and Ba–Al–Ti–O produced by aerodynamic levitation and laser heating

2006 J. Phys.: Condens. Matter 18 L407

(http://iopscience.iop.org/0953-8984/18/32/L01)

INSTITUTE OF PHYSICS PUBLISHING JOURNAL OF PHYSICS: CONDENSED MATTER

J. Phys.: Condens. Matter **18** (2006) L407–L414 doi:10.1088/0953-8984/18/32/L01

LETTER TO THE EDITOR

Novel behaviour and structure of new glasses of the type Ba–Al–O and Ba–Al–Ti–O produced by aerodynamic levitation and laser heating

L B Skinner[1], A C Barnes[1] and W Crichton[2]

[1] HH Wills Physics Laboratory, Tyndall Avenue, Bristol BS8 1TL, UK
[2] European Synchrotron Radiation Facility, 6 rue Jules Horowitz, BP 220, Grenoble Cedex, F-38043, France

E-mail: a.c.barnes@bristol.ac.uk

Received 7 July 2006
Published 24 July 2006
Online at stacks.iop.org/JPhysCM/18/L407

Abstract

Novel barium aluminate ($BaAl_2O_4$) and barium alumino-titanate ($BaAl_2TiO_6$) glasses have been produced by aerodynamic levitation and laser heating. $BaAl_2O_4$ forms a clear and colourless glass under containerless and rapid quenching conditions. Under similar rapid quenching conditions $BaAl_2TiO_6$ forms an opaque and black glass, while under slower and controlled quenching conditions it is possible to form a clear and colourless glass. The formation of the opaque or clear glass is reversible and purely dependent on the quench rate used. By slowing the quench rate further, it is possible to produce a milky glass suggestive of liquid–liquid phase separation in the liquid before glassification. High-energy x-ray diffraction experiments confirm the glassy state of these materials and show coordination structures and bond distances similar to their crystalline analogues.

1. Introduction

In recent years, aerodynamic levitation and laser heating techniques have been used to produce glasses under containerless and rapid quenching conditions. The absence of nucleation centres and contamination caused by the use of a container means that glasses can be produced by this method that cannot be produced by conventional quenching techniques (Zhang *et al* 2003). In this paper we report on two new glasses, based on the $BaO–Al_2O_3$ and $BaO–Al_2O_3–TiO_2$ systems that we have produced using these methods.

Recent aerodynamic levitation experiments have shown that it is possible to produce $NdAlO_3$ and $CaAl_2O_4$ glasses relatively easily using levitation methods. These materials are interesting in that the Nd^{3+} and Ca^{2+} ion have the same ionic radius (0.99 Å) and show some

structural similarities (namely a short metal–oxygen distance at ∼2.5 Å and longer metal–oxygen distance at ∼3 Å). It is also well known that, on moving along the lanthanide series, the size of the rare-earth ions decreases (the lanthanide contraction). In the rare-earth and yttrium aluminate glasses ($REAlO_3$, where RE is the lanthanide or Y) this contraction is used to explain the decrease in their glass forming ability. For example, for Y_2O_3–Al_2O_3 and Er_2O_3–Al_2O_3 glasses the material quenches to a two-phase glass (Aasland and McMillan 1994, Tangeman *et al* 2004 and Weber *et al* 2000). However, no observations of the effect of *increasing* ion size on the glass-forming properties of the systems have been made. The Ba^{2+} ion has considerably larger size than Ca^{2+}, with a radius of 1.34 Å, and hence the structure and glass-forming ability of Ba-containing glasses should provide useful insight into this question as well as to the behaviour of the aluminate glasses in general. In addition, materials based on Hollandite—$Ba_3TiAl_{10}O_{20}$—are important technological materials, in the form of SYNROC, for the encapsulation of highly active nuclear waste (Ringwood *et al* 1979). At the present time, the developments are mainly in the form of glass ceramics where waste loaded SYNROC is encapsulated in a glass matrix. The ability to form glasses from this material, especially with regard to their ability to encapsulate large active ions, may be of future relevance to these waste storage technologies. In this letter we present x-ray diffraction measurements of the structure of $BaAl_2O_4$ and $BaAl_2TiO_6$ glasses produced by aerodynamic levitation and laser heating and compare them to the structure of other pure aluminate glasses.

2. Experimental methods

An aerodynamic levitation system supplied by Containerless Research Incorporated (CRI, Evanston, IL, USA) was used to produce glasses of the composition $BaAl_2O_4$ and $BaTiAl_2O_6$. In each case equimolar quantities of finely powdered and carefully dried BaO and Al_2O_3 ($BaAl_2O_4$) and $BaTiO_3$ and Al_2O_3 ($BaTiAl_2O_6$) were thoroughly mixed and rapidly melted by laser heating on a copper hearth to form small polycrystalline samples of the basic material with a typical diameter of 2 mm. These samples were then levitated on a pure argon gas stream in the levitator and melted, by heating with a CO_2 laser, to form aerodynamically levitated liquid spheres at temperatures of up to 2500 K. After allowing the samples to equilibrate for a minute, they were quenched by reducing the laser power and allowing the sample to cool in the argon levitation gas stream. The fastest quench rate obtained was by instantaneously switching off the laser and corresponded, for a sample of ∼2 mm diameter, to a quench rate of ∼200 K s^{-1}. Slower and more controlled quench rates were obtained by linearly ramping the laser power downwards under direct computer control. The temperature of the sample, as recorded using a Mikron M90V pyrometer, was continually measured as a function of time in all cases. Using this technique, controlled and reproducible quench rates between 10 and 200 K s^{-1} were obtained in the experiment. No evidence of strong recalescence of the supercooled liquid (indicative of crystallization) was observed for the materials produced. High-energy x-ray diffraction at an energy of 61.332 keV (the Yb K edge corresponding to a wavelength of $\lambda = 0.22$ Å) was carried out using the ID27 beamline at the European Synchrotron Radiation Facility (ESRF). The incident x-ray beam was set to a height of 0.3 mm and was set to pass directly through the centre of the sample sphere. For the $BaAl_2O_4$ sample, the data was collected using the instrument oscillating collimator system and image plate detection. This gave a restricted angular range corresponding to a Q range of $\sim 1.0 < Q < 11$ Å^{-1}. For the two $BaTiAl_2O_6$ samples, the measurements were made using a vertical detector arm moving between $2^\circ < 2\theta < 60^\circ$ to give a wider Q range of $\sim 1.0 < Q < 30$ Å^{-1} but at the expense of a reduced count rate.

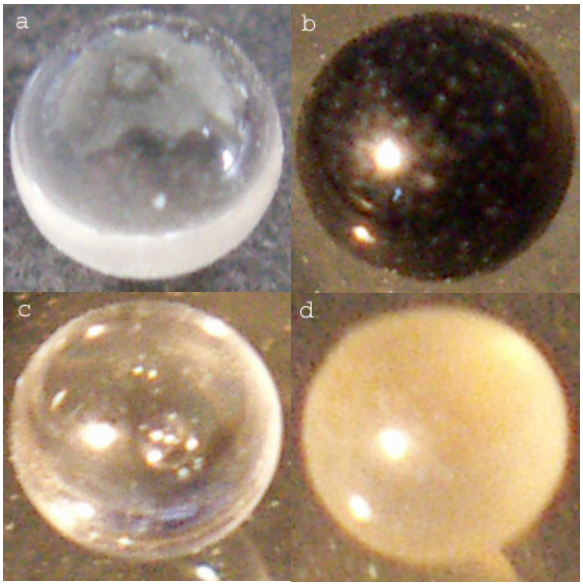

Figure 1. Photographs of glass samples of (a) $BaAl_2O_4$, (b) rapidly quenched $BaTiAl_2O_6$ ($\sim$200 K s^{-1}), (c) slowly quenched (50 K s^{-1}) $BaTiAl_2O_6$, and (d) very slowly quenched ($<\sim$20 K s^{-1}) $BaTiAl_2O_6$.

(This figure is in colour only in the electronic version)

3. Results

Several samples of each material were produced under identical processing conditions to confirm the reproducibility of the production method. Figure 1 shows photographs of some of the samples produced. Photograph (a) is pure $BaAl_2O_4$. This was produced at the fastest quench rate possible by directly cutting the laser power heating the sample. The resulting sphere was perfectly clear and transparent. At slower quenching rates, strong recalescence was observed and the sample formed a polycrystalline and opaque white sphere. Photographs (b), (c) and (d) are of the identical composition $BaTiAl_2O_6$, but have been produced using different quench rates. Sample (b) is black and opaque and was produced at the fastest possible quench rate by instantaneously cutting the laser power. Sample (c) was produced using a quench rate of 50 K s^{-1} and was clear and transparent with a slight brown discolouration. It should be noted that it is possible to produce these black opaque or clear transparent states reliably and repeatedly for the *same* sample solely by changing the quench rate used. For intermediate cooling rates, the sample formed a pale to dark brown glass. Sample (d) was produced by using a quench rate of less than 20 K s^{-1} and has a white 'milky' appearance, suggesting that some phase separation has taken place. Figure 2 shows the x-ray diffraction patterns of samples of (a), (b) and (c) recorded at the ESRF. At this energy, the attenuation length of the x-rays into the material is greater than 0.5 mm for both samples, so the x-rays are probing the bulk glass and not the surface. There is no evidence of any crystallization in any of the samples. All the structure factors show a prominent peak at $Q \sim 2$ Å^{-1} with a smaller second peak at $\sim$2.6 Å^{-1} with oscillations observable out to $\sim$10 Å^{-1}. Figure 3 shows the experimental normalized x-ray total radial distribution function $g_{\mathrm{NX}}(r)$ given by:

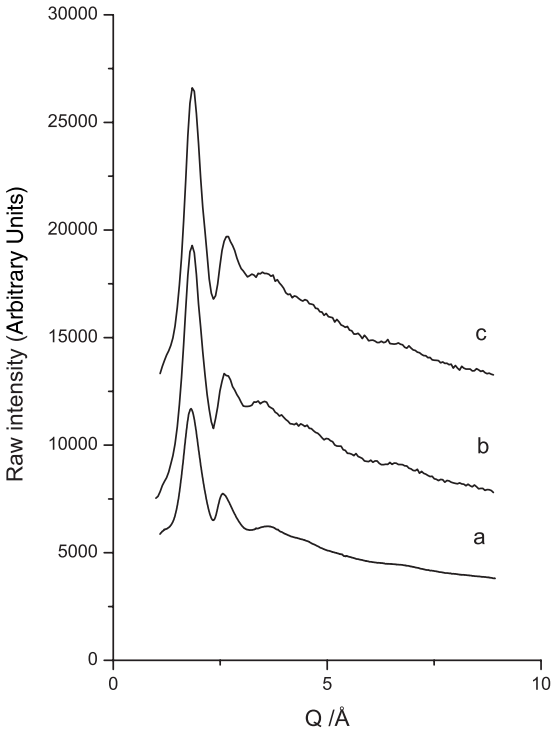

Figure 2. The uncorrected x-ray diffraction patterns of (a) $BaAl_2O_4$, (b) rapidly quenched $BaAl_2TiO_6$, and (c) slowly quenched $BaAl_2TiO_6$.

$$g_{\mathrm{NX}}(r) - 1 = \frac{1}{2\pi^2 \rho_{\mathrm{N}} r} \int \frac{\sum_{i=1}^{N} \sum_{j}^{N} c_i c_j f_i(Q) f_j(Q) Q(S_{ij}(Q) - 1) \sin(Qr)}{\sum_{i=1}^{N} \sum_{j=1}^{N} c_i c_j f_i(0) f_j(0)} \mathrm{d}Q \tag{1}$$

and the Faber–Ziman normalized total radial distribution functions, $g_{\mathrm{FZ}}(r)$ given by

$$g_{\mathrm{FZ}}(r) - 1 = \frac{1}{2\pi^2 \rho_{\mathrm{N}} r} \int \frac{\sum_{i=1}^{N} \sum_{j}^{N} c_i c_j f_i(Q) f_j(Q) Q(S_{ij}(Q) - 1) \sin(Qr)}{\sum_{i=1}^{N} \sum_{j=1}^{N} c_i c_j f_i(Q) f_j(Q)} \mathrm{d}Q \tag{2}$$

obtained after correcting the data for polarization, scattering volume and absorption. Here, c_i and $f_i(Q)$ are the atomic concentration and (complex) form factor for species i, and ρ_{N} is the atomic number density of the glass. For the case of $BaAl_2O_4$, the maximum Q used for the Fourier transform was 11 $\mathrm{Å}^{-1}$ (the maximum Q available) and for $BaTiAl_2O_6$ it was 20 $\mathrm{Å}^{-1}$ (due to the noise on the data at higher Q). The densities of the samples were calculated from the sample diameters and their measured masses and were found to be 4.0 ± 0.1 and 4.7 ± 0.1 g cm^{-3} for $BaAl_2O_4$ and $BaTiAl_2O_6$, respectively. This gives rise to corresponding atomic number densities of $\rho_{\mathrm{N}} = 0.066$ and 0.093 $\mathrm{Å}^{-3}$, respectively.

In the $g_{\mathrm{FZ}}(r)$ representation, the broadening of the peaks in real space due to the Q-dependent form factors is reduced considerably at the expense of errors due to the different Q dependences of the form factors. However, this representation does allow for the better resolution of the peaks in $g(r)$. For the case of both $BaTiAl_2O_6$ glasses, clear peaks are observed in $g_{\mathrm{FZ}}(r)$ at $r = \sim 1.8, 2.8$ and 3.6 Å. The peak at $\sim$3.6 Å is asymmetric, with

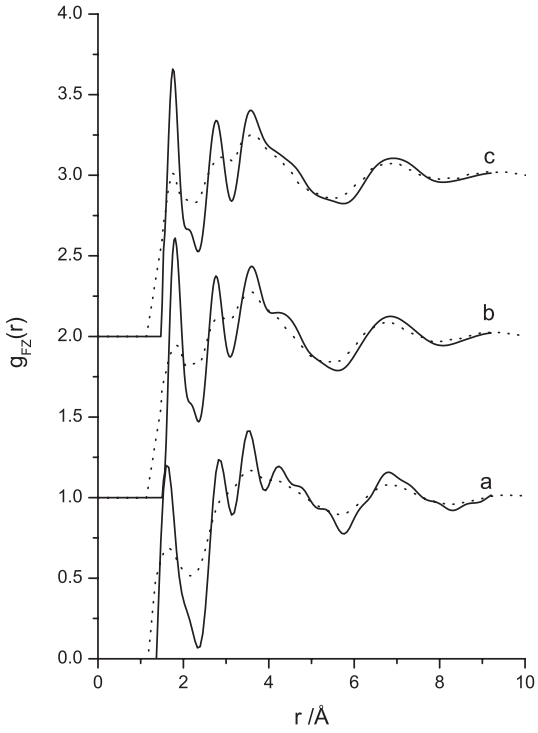

Figure 3. The normalized $g_{NX}(r)$ (dotted lines) and $g_{FZ}(r)$ (full lines) for (a) $BaAl_2O_4$, (b) rapidly quenched $BaAl_2TiO_6$, and (c) slowly quenched $BaAl_2TiO_6$.

two shoulders on the high r side at ∼4.2 and ∼5 Å, respectively. Finally, a further strong peak is observed at 6.8 Å. For the case of the $BaAl_2O_4$ glass, the resolution in real space was limited by the Q-range of the data taken. However, a peak was again observed at 1.8 Å, with further peaks at ∼2.8, 3.5, 4.3 and 6.8 Å.

4. Discussion

The complete absence of Bragg scattering in the x-ray diffraction patterns obtained in this work confirm that all of the materials that we have produced are true glasses. The $BaTiAl_2O_6$ glass is unusual, as it shows strong changes in its physical appearance depending on the quench rate used. The black opaque nature of the rapidly quenched sample suggests the formation of a large number of defects in the sample, giving rise to a strong optical absorption. Such discolouration has been observed in glasses containing TiO_2 before, and is attributed to the partial reduction of TiO_2 to liberate free oxygen into the structure (Cheng and Chen 1986). The change to a clear and transparent glass at slower quench rates suggests that, on these timescales, this free oxygen has time to recombine to leave a defect-free and optically transparent material. The production of samples with a 'milky' appearance has been observed previously with samples produced by aerodynamic levitation, most notably in Y_2O_3–Al_2O_3 and Er_2O_3–Al_2O_3 glasses, and is explained as being due to microscopic phase separation of the liquid into two liquid phases that quench into two distinct types of glass (Weber *et al* 2000). We believe that similar behaviour is occurring in the $BaTiAl_2O_6$ sample. We did not carry out x-ray experiments on this glass for this reason.

A discussion of the structure of these glasses is best approached with reference to the structure of some of their crystalline analogues. Huang *et al* (1994) have reported the crystal structure of $BaAl_2O_4$ as hexagonal $P6_3$ with unit cell parameters of $a = 10.32$ Å and $c = 8.72$ Å. The structure is characterized as interconnected $[AlO_4]$ tetrahedral, with the barium atoms lying in the spaces between them. A comparison of the peak positions and intensities of the glass with the interatomic distances and peak intensities of the crystal shows strong similarities and suggests that the glass is similarly composed of interconnected $[AlO]_4$ tetrahedra with non-bridging Ba ions.

A crystal structure for the composition $BaTiAl_2O_6$ has not been published. However, various alumina-rich compounds containing these elements exist, for example the Hollandite structure $Ba_3TiAl_{10}O_{20}$ (Fallon *et al* 1985, Cheary 1986) and $BaTiAl_6O_{12}$ (Cheary 1986). These are complicated structures characterized by interconnected Al–O tetrahedra and octahedra and Ti–O octahedra that form a three-dimensional framework in which the large Ba ions occupy the spaces (tunnels) in between. In all of these structures, the Al–O distance lies in the range 1.70–1.85 Å and the Ti–O distance typically lies in the range 1.80–2.00 Å. We therefore associate the strong first peak in $g(r)$ in these glasses with these distances. However, it is not possible to resolve these peaks separately, although a shoulder on the first peak is observed at about 2 Å that may be associated with some Ti–O correlations. By a similar comparison with the crystals, the broad peak at ∼2.8 Å is dominated by the Ba–O, Ti–Ti, Al–Al and Ti–Al distances, with a weak contribution (due to its low atomic number) from the O–O distance at 2.8 Å. The peak at ∼3.6 Å can be associated almost exclusively with the Ba–Ti and Ba–Al distances and the small shoulder at ∼4.2 Å with the Ba–Ba distance. Therefore the diffraction pattern of the glass, at this level, is consistent with the packing of Al–O and Ti–O in a similar fashion to the crystal.

The high atomic number of barium (56) is the reason for the dominance of the Ba–X correlations in the 3.2–5 Å range. A closer inspection of the $S(Q)$ and $g(r)$ of the dark and clear $BaTiAl_2O_6$ shows that there are subtle differences between the two; namely a small shift in the peaks in $S(Q)$ to smaller Q for the clear sample that manifests itself as changes in the positions and shapes of the peaks in $g(r)$. The first peak $g_{NX}(r)$ for the clear sample is slightly sharper than the black sample. This difference in sharpness is clearly observable in $g_{FZ}(r)$ if the maximum Q of 30 $Å^{-1}$ is used for the Fourier transform at the expense of a large number of transform 'ripples' produced by noise on the data at high Q. This observation suggests that the black sample may be considered in some sense 'more disordered' than the clear sample; consistent with the presence of a large number of defects and vacancies in the structure. On the other hand, the sharper and stronger peak in the clear sample indicates that the slower quench rate has allowed more time for atoms in the melt to find their chemically favourable positions. Differences between the two samples may also be observed for the peak at ∼4.2 Å, suggesting that some reordering, on slower quenching, is also taking place on the intermediate length scales.

To date, relatively few pure aluminate glasses have been produced that do not include an additional network former such as SiO_2. Hannon and Parker (2000) reported neutron diffraction measurements on an analogous system, $CaO–Al_2O_3$, but reported that they were only able to make glasses up to the composition 38 mol% CaO by traditional rapid quenching techniques. Benmore *et al* (2003a) reported neutron and x-ray diffraction studies of calcium aluminate glasses at 50 and 64 mol% CaO produced by aerodynamic levitation and laser heating methods. Weber and co-workers (Weber *et al* 2000) similarly produced a range of rare-earth aluminate glasses at up to 50 mol% RE_2O_3, where RE is the rare earth. It is noted that, in these systems, the lighter rare earths (such as Nd, which has the same ionic radius as Ca) forms a glass relatively easily, but the heavier rare earths such as erbium are difficult to glassify and prone

to glass–glass phase separation. It is suggested that this trend is due to the decrease in size of the rare-earth ion in accordance with the known lanthanide contraction. In a neutron diffraction and isotopic substitution experiment, Benmore *et al* (2003b) reported the structure around Nd in $NdAlO_3$ glass obtained by neutron diffraction and isotopic substitution. It is interesting to compare their observations with the glasses studied here. In our case, as already noted, the Ba-related structure is very apparent in the total $g(r)$ due to the high atomic number of barium. As expected, given the ionic diameter of Ba^{2+} (1.34 Å), we find no evidence of any Ba–O peaks below ∼2.8 Å, in contrast to the Nd and Ca glasses, where two M–O distances were observed at ∼2.5 Å (corresponding to the Nd^{3+} and Ca^{2+} radius of 0.99 Å) and a less prominent distance at ∼3 Å. The comparatively large size of the Ba ion therefore does not appear to inhibit glass formation. Benmore *et al* also observed a lack of Nd-related structure on intermediate length scales (3–5 Å). This is in contrast to the results that we see for the $BaAl_2O_4$ and $BaAl_2TiO_6$ glasses, which show strong peaks on these length scales due to the Ba–Ba, Ba–Ti and Ba–Al correlations.

Finally, crystalline barium alumino-titanates and related compounds known as SYNROC are seen as alternatives to borosilicate glass for the encapsulation of some forms of high-level nuclear waste. This is due to their ability to immobilize a large number of the active ions produced during nuclear energy production. In this work we have demonstrated that it is possible to form glasses from compositions similar to SYNROC. This suggests that it may be possible to combine the advantages of encapsulation in glass (no grain boundaries etc) with the advantageous properties of the aluminates (high waste product loading) to form new glasses or glass ceramics for the storage of nuclear waste.

We therefore believe that these barium aluminate glasses are worthy of further, more detailed, study to observe the effect of the ion size and composition on the glass stability and structure. In this respect, it would also be interesting to look at the strontium analogues of these glasses, as the ionic radius of the Sr^{2+} ion lies in the intermediate range between that of Ca^{2+} and Ba^{2+}.

5. Conclusions

The results presented here confirm that we have produced two previously unreported glasses based on barium aluminates. The closest analogue to this glass is calcium aluminate, and this barium aluminate glass is of interest in this context, as it may perhaps throw some light on the glass-forming ability of the alkaline earth aluminates with respect to the size of the alkaline earth ion. In this respect, we predict that it should also be possible to produce strontium aluminate glass using these methods. We have also demonstrated the glass-forming ability of pure Ba–Al–Ti–O glasses, and it will be interesting to explore the glass-forming range of these materials with respect to the Al–Ti ratio.

L Skinner would like to acknowledge the UK Engineering and Physical Sciences Research Council (EPSRC) for the award of a PhD studentship. The x-ray diffraction work was conducted by WC using ID27 at the ESRF through the allocation of beam time for in-house research. We wish to acknowledge the use of the EPSRC's Chemical Database Service at Daresbury (Fletcher *et al* 1996).

References

Aasland S and McMillan P F 1994 *Nature* **369** 633

Benmore C J, Weber J K R, Sampath S, Siewenie J E, Urquidi J and Tangeman J A 2003a *J. Phys.: Condens. Matter* **15** S2413

Benmore C J, Weber J K R, Siewenie J E and Hiera K J 2003b *Appl. Phys. Lett.* **83** 4954
Cheary R W 1986 *Acta Crystallogr.* B **42** 229
Cheng J and Chen W 1986 *J. Non-cryst. Solids* **80** 135
Fallon G D, Gatehouse B M and Wright P J 1985 *J Solid State Chem.* **60** 203
Fletcher D A, McMeeking R F and Parkin D 1996 *J. Chem. Inf. Comput. Sci.* **36** 746
Hannon A C and Parker J M 2000 *J. Non-Cryst. Solids* **274** 102
Huang S-Y, Von Der Mühll R, Ravez J, Chaminade J P, Hagenmuller P and Couzi M 1994 *J. Solid State Chem.* **109** 97
Ringwood A E, Kesson S E, Ware N G, Hibberson W and Major A 1979 *Nature* **278** 219
Tangeman J A, Phillips B L, Nordine P C and Weber J K R 2004 *J. Phys. Chem.* B **108** 10663
Weber J K R, Abadie J G, Hixson A D, Nordine P C and Jerman G A 2000 *J. Am. Ceram. Soc.* **83** 1868
Zhang Y, Navrotsky A, Tangeman J A and Weber J K R 2003 *J. Phys.: Condens. Matter* **15** S2343